MJoSHT
Malaysian Journal of Science, Health & Technology
USIM
[mjosht.usim.edu.my]

Article

A Critical Review of Cu_2SnS_3 (CTS) Thin Films Solar Cells

Md. Fakhrul Islam[1,a],Nadhrah Md Yatim[1,b], Puvaneswaran Chelvanathan [2,c], Mohammad Tanvirul Ferdaous[3], Mohd Azman Hashim@Ismail[1], Anup Kumar Modak [4], Prof. Nowshad Amin[3]

[1]*Faculty of Sciences Islam Malaysia , Universiti Sains Islam Malaysia (USIM), Bandar Baru Nilai,71800, Negert Sembilan, Malaysia*
E-mail: [a]fakhrutitu@gmail.com E-mail:[b] nadhrah@usim.edu.my

[2] *Solar Energy Research Institute (SERI), Universiti kebangsaan Malaysia (UKM),43600, Bangi, Selangor, Malaysia*
E-mail:[c] cpuvaneswaran@yahoo.com

[3]*Institute of sustainable Energy, Universiti Tenaga Nasional (UNITEN),43000, Kajang, Selangor, Malaysia*

[4]*Faculty of Engineering, Daffodil International University, Ashulia, Dhaka, Bangladesh*

Abstract— **To increase energy demand, reliability, and increasing efficiency, thin-film solar cells get the main focus. Various types of solar cell like (Cu(In,Ga)Se_2 (CIGS), Cadmium telluride (CdTe) and copper zinc tin sulfide (CZTS) based absorber compound now eliminated by CTS (Cu_2SnS_3) for different reason like toxicity, shortage and structural complexity. Focus on CTS is increasing because it is nontoxic and it is environmentally friendly. CTS-based solar cell's power conversation efficiency increases and 30% theoretical efficiency indicates it's developing sign. For analyzing the synthesis property, X-ray diffraction (XRD), Raman, Energy Dispersive X-ray (EDX), X-ray fluorescence (XRF) techniques are used. For the synthesis of thin-film solar cells like CTS, different physical methods are used among all sputtering methods. The electron beam evaporation vacuum evaporation method has exposed better efficiency and high product quality and reliability. Additionally, the composition, variation of thickness, structural defects, and elemental composition make the absorber layer's quality affect the performance. This paper has discussed the annealing treatment of CTS-based solar cell synthesis, and it's essential to improve the thin film properties of thin films. This paper describes the reason for efficiency reduction also the scope for future research.**

Keywords— **CTS, Thin Film, Solar Energy, Thin-film solar cell, Sputtering.**

I. INTRODUCTION

To meet the increasing energy demand, solar energy is the most promising solution to meet present and future energy demand. For increasing efficiency and decreasing cost solar cell is now in trading. It is a semiconductor material that's initiate electrical energy [1]. Now photovoltaic-based solar cells produce one percent of words energy production [2]. Now solar cells based on crystalline silicon reach power conversion efficiency PCE 26.7% [3] though thin-film is in a remarkable position because it uses less raw material. Within thin-film solar cells, PCE is 22.1% and 22.6% for CdTe and CIGS-based solar cells, including low-temperature coefficient[3, 4]. CIGS production depends on a rare element like Se and Ga. Due to lacking the raw material it can't use for hug use also price can increase suddenly [5]. For Cadmium telluride (CdTe), Cd is more toxic, and beside Tellurium is comparatively rare. So the researcher focused on the environment-friendly solar cell. For this, CTZS is an example. Its material and property of bandgap is the same as CTS. However, the power conversion efficiency is significantly less than CdTe and CIGS [2]. CTS absorber layer is environmentally friendly; beside that it is low cost and it's raw material are available. CTS is a P-type semiconductor that's contains high coefficient absorption coefficient of about 104 cm^{-1} [5], and also it has a tunable bandgap (1.1-1.5eV) that is effective for photovoltaic absorption [2]. The technological status of CTS thin films are shown in Table I.

The current highest PCE of CTS is 4 to 6%. Theoretical efficiency is about 30%, which is quite high [2]. Hence the

TABLE I
TECHNOLOGICAL STATUS OF CTS THIN FILMS

Process	Authors	Deposition Method	η (%)	Voc (mV)	Jsc (mA/cm^2)	FF (%)
Vacuum	[6]	Sputtering	3.05	243	26.2	47.9
	[7]	Sputtering	0.76	215	13.8	25.5
	[8]	EBE	1.20	134	27.9	31.2
	[9]	EBE	2.70	244	29.0	38.5
	[10]	EBE	2.54	211	28.0	43.0
	[11]	Evaporation	3.66	248	33.5	43.9
	[12]	Evaporation	4.29	258	35.6	46.7
	[13]	Evaporation	4.63	283	37.3	43.9
	[14]	PLD	0.82	260	11.90	24.0
Non- vacuum	[15]	ED	2.84	249	29.3	39.0
	[16]	ED	0.54	104	17.1	30.4
	[17]	Ball milling	1.92	320	23.4	28.0

best efficiency of Na doping on CTS was found 4.6%[12]. Moreover, Umehara et al. reported that Ge-induced CTS had achieved the highest PCE, 6.7%, with changing bandgap structure using the co-sputtering method[18]. Physical and chemical both method of synthesis is applicable for CTS based solar cell. Including physical method sputtering [2], E-beam evaporation [8], Coevaporation [19] , ball mill [17] etc. For chemical method electrodeposition [16], SILAR (successive ionic layer adsorption and reaction) [20], spray pyrolysis [21], etc. are most common. Physical methods are costly and more complex, but its final product is pure so use of physical method is more perfect [2, 5]. However, the chemical methods are cheaper and very little material waste, so the chemical method is also better for production in another logic. So it is clear that both methods have benefits depends on the expected outcome. Annealing treatment processes has a vital role in increasing efficiency [2]. PCE, Open circuit voltage(Voc), short circuit current density (Jsc), fill factor(FF) of CTS thin-film solar cell depends on bandgap, crystal structure, annealing temperature along with synthesis process [3, 22]. This study focuses on the PCE of CTS by analyzing different physical and chemical methods with various parameters.

II. CTS Properties

A. *Crystal structure*

The CTS has various phases like cubic, tetragonal, orthorhombic, monoclinic, and triclinic, which were reported [23-26]. The varying degrees of disorder on the cation sublattice were representative of the different crystal structures recommended by [26], as shown in Fig I. The various phase variations are introduced from the octet rules, ensuring the lowest energy level of a stable compound.

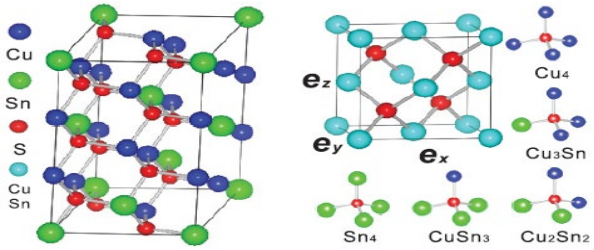

Fig I: CTS crystal structure a) monoclinic structure b) cubic structure and Cu_4, Cu_3Sn, Cu_2Sn_2, $CuSn_3$ or Sn_4 Structure.

CTS's five tetrahedral coordination is possible as an anion such as Cu, Cu_3Sn, Cu_2Sn_2, $CuSn_3$, and Sn_4. However, those were unsatisfied with the octet rule[26], which shows that the charge-neutral CTS compound, the anion atoms with 1:2 ratio can exist surrounding $Cu_2Sn_2$and Cu_3Sn clusters. The formatted of different CTS phases results from a long-range disorder of anion, while the short-range disorder anion well defined stable compound. The zinc blende structure resulting from full anion disorder results in a cubic unit cell, a zinc blende structure with a partial disorder created tetragonal structure, and Zinc blende structure with full disorder crested monoclinic structure. Each of the phases had a structural and associated composition variation expected to induce different splitting mechanisms and wave-orbital overlapping. As a result, a wide range of varying in the concomitant optoelectronic properties and electronic band structure include absorption coefficient, electron affinity, and bandgap [23, 24, 27]. The preferential texturing estimation for cubic phase CTS are shown in Table II. Zhai et al. was analyzed that CTS exists only cubic, monoclinic, and tetragonal structures[26].

TABLE II
PREFERENTIAL TEXTURING ESTIMATION FOR CUBIC PHASE CTS

Plane (h k l)	Reference value	Experimental value	Reference value	Experimental valve
(111)	28.4467	28.4435	100	100
(200)	32.9638	32.9654	13.61	6.73
(220)	47.3104	47.2854	47.75	45.56
(311)	56.1314	56.0780	29.73	11.68
(311)	76.3896	76.3553	8.70	3.04
(422)	88.0470	88.0130	8.81	1.71

The XRD has mainly been utilized to determine the product's phase purity like CTS's structural characterization. The Fernandes et al. showed that the tetragonal structure had the ratio c/a close to 2 (a = 5.41Å and c = 10.81Å) whereas cubic CTS had a lattice parameter of a = 5.43Å [23]. In this study also provide detail comparison cubic and tetragonal structure of preferential texturing of data, which are shown in Table III.

TABLE III
PREFERENTIAL TEXTURING ESTIMATION FOR TETRAGONAL PHASE CTS

Plane(h k l)	Reference value	Experimental value	Reference value	Experimental Value
(112)	28.5398	28.5656	100	100
(200)	33.0703	33.1398	13.21	4.75
(204)	47.4725	47.5070	45.95	44.17
(312)	56.3246	56.3369	27.73	12.34
(316)	76.6807	76.8577	7.61	1.74

The ICDD reference number for cubic, tetragonal, and monoclinic were claimed as 01-089-2877, 01-089-4714, and 01-070-6 338, respectively, elsewhere space group of this phases were marked as F-43m, I-42m, and C1c1, respectively [7, 23]. Using XRD analysis, the sample were assigned as the plane of (1 1 2), and (-1 3 1), respectively where as the dominant peak positions for the cubic, tetragonal and monoclinic were found as 28.45 0, 28.58 0, and 28.50 0, respectively [23]. Although CTS were also found the other characteristics peaks at 33.5^0, 47.5^0, and 56^0 at the 2θ position [11, 12, 19, 23, 28, 29].

The CTS structure major peaks like cubic, tetragonal, and monoclinic are originated at very near to 2θ values, it's made difficult to the structural phase differentiate. Secondly, the same CTS cubic structure can exist in the Cu_3SnS_4 impurity phase and detecting the lattice parameters is sufficient. Therefore, the XRD has the detection limit in the range within 1-5%, and the effect of the optoelectronic properties of the material could include impurity phases in lower concentrations.

Raman study was used as a supplement that XRD analysis alone cannot identify the phase ambiguity of CTS thin film as well as those in recent studies published in the last several years. The Raman spectra when used to identify the crystal structure of CTS then its peak don't overlap like as XRD peaks. Therefore, CTS or cu-Sn-S phases have no theoretical work to calculate the Ramon active modes. Though, there is no disagreement in the field about the exact peak position of different phases because phase assignment is empirical. Raman's studies analyzed cubic, tetragonal and monoclinic phases that are listed in Table IV. almost all phases have Raman mode near the shift of 350 cm^{-1}, source of data shown in Table IV, and the analogy of CZTS is assigned as A_2 mode [30, 31].

Moreover, the different phases are the varied prime mode of Raman study. For the CTS, tetragonal and monoclinic is the found value 336 and 290 cm^{-1}, as well as for the cubic CTS active Raman mode (A_1) is located at 303 cm^{-1}. Although, Ramon's study is important to point out the CTS phase for the different active Raman modes (A1), in the distinct phases. Moreover, by combining Raman and XRD have been achieved for accurate phase identification. Recently, for the characterization, another study has been used X-ray photoelectron spectroscopy (XPS) to the oxidation state of each element. This data can help verify phase purity [14].

B. Compositional and morphological properties

The most important parameter of CTS thin film is controlling by the Cu/Sn ratio. The prepared CTS can be either Cu-poor state (Cu/Sn<2), Cu-rich state (Cu/Sn>2), or stoichiometric state (Cu/Sn=0) using based on Cu/Sn = 0.

TABLE IV
REPORTED RAMAN STUDY DATA FOR DIFFERENT CTS PHASES

Raman Peaks Shift (cm^{-1})	Assigned Phase	Sources
303,355	Cubic	[23]
303,355	Cubic	[20]
335,351	Tetragonal	[32]
336,337,351	Tetragonal	[23]
297,337,352	Tetragonal	[33]
295,337,354	Tetragonal	[34]
285,332	Tetragonal	[19]
290,352,314 (weak), 374 (weak)	Monoclinic	[6]
290-295,354-357,314 (weak), 374 (weak)	Monoclinic	[35]
292,349,255 (weak)	Monoclinic	[11]
290,352	Monoclinic	[13, 36]

Although, in terms of sulphur (S) content, CTS thin film can be again divided as S-rich state (S/metal>1) and S- poor state (S/metal<1). Zhang et al. was stated that CTS thin-film solar cell is not able to getting high efficiency in Cu-rich state [37]. The stoichiometric state of CTS has found the same scenario in the absorber layer. In contrast, Cu-poor state, Cu-rich state were obtained the comparatively most high efficiency (U-2013, N-2015, K-2015). The high efficiency was attributed to formation of Cu-vacancy (V_{cu}) as a result of lack of Cu atoms that is actually an acceptor type of defect as well as physical explanation.

C. Optical properties

Multiple theoretical works have calculated CTS thin films' bandgap in the range of 0.84-0.88 eV [26, 27]. However, the experimental results revealed that band gap of CTS could vary from 0.83-0.177eV [17, 38]; nevertheless, most often, this value has been found constant in the range of 0.86-1.02 eV, which was similar to the reported theoretical value [10, 28, 34, 39, 40]. Zhang et al. (2014) reported a route to produce highly crystalline CTS thin films through sulphurization of sequentially sputtered Sn –rich precursors. Cu/Sn strucked precursors were preheated at 200 ^{o}C for 4hr under vacuum (10-03 Pa) followed by sulphurization of samples at 560 ^{o}C for 2 hr. cubic CTS phase was formed with a bandgap of 1.35 eV [37]. Dong et al. (2015) fabricated CTS thin films with sulphurization temperature variation from 400 to 500 ^{o}C. They observed the effect of elevated sulphurization temperature in terms of crystallinity, chemical composition, and optical bandgap. The higher sulphurization temperature can be attributed to better crystallinity and proper chemical composition of CTS thin films. The optical band gap was measured asn0.92 eV, 0.96eV, 0.98 eV and 099eV for the sulphurization temperature of 400 ^{o}C, 450 ^{o}C, 500 ^{o}C, 550 ^{o}C etc [39].

Similar to temperature, sulphurization time affects the optical properties of CTS thin films. Dong et al. (2015) reported the correlations of sulphurization time and CTS thin-film S properties. They have deposited metallic precursors with sulphurization for 5 to 30 min atm 575 oC in a nitrogen environment. The cubic phase was identified for each sulphurized sample having ICDD card no 01-089-2877 [39]. However, the change bandgap was measured as 1.02 eV, 1.01 eV, 1.00eV, and 0.98 eV, for the sulphurization time for 5min, 10min, and 30min, respectively.

D. Electrical properties

CTS's probable antisite defects are Cu_{zn}, $Zn_{cu,}$ and the defects states V_{cu}, V_{zn}, Vs as vacancy defects. Hence CTS works as a p-types semiconductor, whereas the acceptor type of defect V_{cu} is the lowest defect [41]. The Cu atom deficiency indicates that cu poor is an important condition to fabricate CTS solar cells successfully.

The electrical properties of CTS is varied in different literature, which was reported significantly. The resistivity of CTS material was measured at any point between 0.0004 to 10 Ω–cm [23, 34]. Small amounts of conductive material phases such as Cu4SnS4 and Cu2S incorporated impurities during various processing steps, and the different synthesis conditions vary the intrinsic defect concentration. Therefore, The CTS is always reported as a p-type semiconductor in the absorber layer, and the carrier concentration ranging from 10^{17} to 10^{21} 1/cm^3 [6, 24]. However, the value of carrier concentration is very high related to photovoltaic absorber materials. The majority carrier mobility characterization has to get value from 0.03-22.3 cm^2/Vs using Hall Effect measurement [28, 33]. Therefore, there does not seem to be an important correlation between the grain size (using SEM) and the majority carrier mobility because the means free path is limited by defects within the grain [20].

The conduction mechanism of CTS has been made to understand to need several steps. The electrical conductivity has been measured between the room temperature to 85K as well as observed to different conduction regimes [42]. According to Arrhenius's law, the relationship of the electrical conductivity and temperature can be fit above 238K, and is pointed to thermal excitation charge carriers. According to Mott's law, the data can be fit below 238K, indicating the variable range hopping mechanism [43]. Similarly, Dias et al. (2014) reported that the transition temperature is 275K. Differently, Tiwari et al. observed three types of conduction regimes: Mott variable range hopping from 5-50K transport is dominated, nearest neighbour hopping from 50-150 K, and thermionic emission over grain boundaries from 150-290K [44]. Therefore, Tiwari et al. have a second work analyzed that in terms of oxygen defects, the change in transport behaviour in their film results from annealing in the air [45].

E. Basic structure of CTS TFSC

The schematic structure of the CTS solar cell is shown in Fig. II. For the deposition of a CTS solar cell, soda-lime glass (SLG) is used as a substrate. Molybdenum (M_o) thin film with a thickness of 1.2 to 1.5µm is sputtered on a glass substrate as back contact because Mo is stable in harsh reactive conditions such as sulpur- containing vapour and high temperature. The absorber layer of p-types CTS thin-film coated Mo thin film thickness from 1.0 to 2.5 µm.

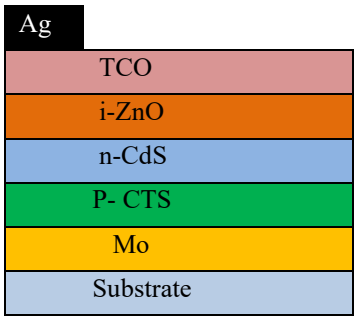

Fig. II Schematic diagram of a typical CTS Solar cell

III CTS FILM DEPOSITION TECHNIQUE

Fuku and Fakoluju have successfully fabricated the first CTS thin-film solar cell in 1987 using various techniques [38]. The two major methods used for the fabrication of CTS thin-film solar cells are the Vacuum deposition technique and Non – vacuum deposition technique.

A. Vacuum deposition technique

The vacuum deposition is a one-of-the-way fabrication that has a semiconductive batter process and large grain size. The two most important vacuum-based methods are evaporation and sputtering, notable for fabrication for the efficient CTS thin-film solar cell. However, the pulse laser deposition process (PLD) is also a vacuum base deposition.

1) Evaporation

Evaporation is one of the established vacuum thin-film deposition methods. The CTS thin film was fabricated first time by using a direct evaporation technique[38]. The efficiency 0.11% was reported using in the schottky –type solar cell, where short-circuit current 0.3mA, the open-

circuit voltage 170 mV, and a fill factor of 0.48. Using electron beam deposition technique by Chino et at was fabricated CTS thin-film solar cell [10]. They used the deposition of elemental Cu and Sn sequentially as a precursor. After the deposited film, they were annealed in the S and nitrogen (N) atmosphere for 2 hr at different temperatures from 450 ^{0}C to 580 ^{0}C to determine the optimum annealing temperature. CTS solar cell's best efficiency was getting 2.70%, and the produced a large grain size at 550 ^{0}C, leading to a decrease in grain boundaries. The effect of the CTS solar cell performance was deposited on the Cu/Sn ratio, using electron beam deposition technique [9]. This study was deposited a wide range of sample varied from 1.39 to 2.22 and sulphurized them at 560 ^{0}C for 2 hr. The most efficient cell was found for the deposition Cu/Sn ratio of 1.62, and the ratio of Cu/Sn sulphurized samples had been found in the range 1.62 to 2.44, with the PCE of 2.93%.

In the following year, Aihara et al. reported a work using the same vacuum deposition technique (2014). Therefore, this study optimized the sulphurization temperature from 500 ^{0}C – 580 ^{0}C with a 20 ^{0}C step. This study took the deposited ratio Cu/Sn 1.7, and the ratio changed after sulphurization from 1.79 to 1.89 for the variation of temperature from 500 ^{0}C .to 580 ^{0}C. The CTS solar cell was found efficiency 2.7% of 0.15 cm^2 for the sulferization temperature of 580 ^{0}C [40]. Table V summarization of CTS finding for sputtering deposition technique.

The fabrication of CTS thin-film solar cell was reported using the co-evaporation method [11]. Therefore, they optimized the sulferization temperature and optimized Cu/Sn ratio too. The deposited Cu/Sn ratio was taking 1.7 to 1.8, and the sulpharized temperatures from 520 ^{0}C and 580 ^{0}C for 5 min per sample. The best quality of CTS found in terms of efficiency 3.66% at the 570 0C temperature with sulphurized ration Cu/Sn of 1.8 from the area 0.154 cm^2 with the value of Voc, Jsc, and FF were 248mV, 33.5mA/cm2 and 0.44, respectively. After that, the work has also optimized the ratio of Cu/Sn. This study varied the deposited ration 1.80 to 1.98 within the narrow reason and sulphurized them at the efficiency of non-alloyed, non-doped pure CTS thin film was getting 4.29% that is for the Cu/Sn ratio of 1.89. Another group worked in 2015 on CTS thin film using the co-evaporation deposition technique [19, 29, 34, 36]. Moreover, in 2015 Nakashima et al. successfully incorporated Na with the CTS thin-film solar cell and performed a comparison study without Na-doping effect on CTS thin-film solar cell. This study was found that the significant influence regarding CTS thin film and CTS was getting the value of Voc = 283 mV, FF=0.439mA/cm$_2$, Jsc= 38.3 mA/cm^2 and η= 4.63% in the mole ratio NaF/Cu=0.075[13].

2) Sputtering

The sputtering method is one of the best suitable and most controllable techniques for comparative all vacuum-based techniques that might be applied in the thin film production at the commercial level. The first reported CTS thin film using sputtering in the year 2010 by Fernandes et al.[23]. In this study, the sample was sequentially deposited the element Cu and Sn target using dc magnetron deposition during 10 min, whereas the power density of 0.11 Wcm^{-2} and 0.11 Wcm^{-2} respectively. The deposition was carried out working pressure of 6*10^{-6} mbar and 2*10^{-3} mbr, respectively, and Ar atmosphere with a base. The samples were sulphurized at the temperatures 350 ^{0}C, 400 ^{0}C, and 520 ^{0}C in the (S_2 + N_2) atmosphere during 10 min for the sample deposition. In this work, the CTS thin-film device was exhibited in phases like Cubic, Tetragonal, and orthorhombic, identified by XRD and Raman analysis. The orthorhombic phases have the atomic structure Cu_3SnS_4, and the cubic phase has the atomic structure Cu_2SnS_3.

The first CTS solar cell was fabricated using the sputtering technique by Umehara et al. [46]. In this study, they were co sputtered in an argon atmosphere, including working power of 0.5 Pa and using Cu and Sn dc gun at RT. The sulphurized in two different ways of a condition like as at normal (S_2+N_2) atmosphere and with the presence of GeS_2 where the effect of Germanium (Ge) allows in CTS's performance alloying. They got the bandgap of 1.02 eV for the CTS alloy with Ge in a cubic phase that showed the great efficiency of 6.01 % in the ratio of 0.17/0.83 of Ge/Sn ratio, non-alloyed solar cell showed only 2.13%.

In the year 2014, analyzed the optimization of the precursor ratio Cu/Sn using the dc sputtering method. The pressure and power were set to 0.8 Pa and 50 W, respectively, and at the room temperature sequentially to deposited Cu and Sn. The time for Cu deposition was setup during 30 min and the time for Sn layer was to set up 10 to 30 min, whereas the deposited Cu/Sn ratio from 2.7 to 0.86. The Sn rich samples (Cu/Sn<2) showed at 560 ^{0}C for 2 hr after sulphurized the sample whereas the stoichiometric value (Cu/Sn=2) a self- adjustment tend of the ratio Cu/Sn.

The author mentioned that the metallic precursor was sulphurized at high temperature (>550 ^{0}C) during 1hr to produce SnS by re-evaporation of Sn samples the stoichiometric value of Cu/Sn ratio. Although, At first sulphide of both copper and tin was formed during the sulphurization of metallic precursors. The ternary Cu_2SnS_3 is formed and these binary sulphides combine together as well as the sulphurization time increase. The extra Sn portion is evaporated as SnS for Sn-rich precursors. The CTS sulphurized sample in the Cu/Sn ratio is the precursor stoichiometric value for Sn-rich. Therefore, The sample had pinhole on the film surface for the evaporation of SnS caused crack, that selecting the deposition Cu/Sn ratio should be controlled, which should be around suggested by this work.

Three sequential studies were reported regarding the sputtering deposition of CTS thin-film solar cell by Dong et al. [7, 28, 39]. The elemental Cu and Sn were sequentially deposited at room temperature for all studies whereas used RF sputtering power density of 4 Wcm^{-2} and 2 Wcm^{-2}, respectively.

In this study, they optimised the sulphurization temperature from the ranges of 400 ^{0}C to 500 ^{0}C. Hence, the best performance was exhibited the sulphurization temperature at 550 ^{0}C for 20 min, having a direct band gap of 0.99 eV for the CTS cubic phase. This means that the higher sulphurization temperature is beneficial for the fabrication of CTS thin film and the sample showed high efficiency as 0.28%.

TABLE V

SUMMARIZATION OF CTS FOR SDT

Ref.	Deposition	Sulphurization	η (%)	Voc (mV)	Jsc (mA/cm2)	FF (%)	Surface Morph.
[23]	$2*10^{-3}$ mbar sequential	350^0C, 400^0C, 520^0C, 10min	-	-	-	-	Rough surface with small grain size
[46]	0.5 Pa co-sputtering	GeS2,S 5 50^0C,1 5 min	35 5	30 .5	55.6	6.0 1	Large grain size above micrometer
[37]	50W,0.8p a sequential	560^0C, 2 hr	-	-	-	-	Smooth and compact surface
[28]	4,2 Wcm^{-2}, sequential	400^0C to 550^0C 20min	18 0	5. 45	26.1	0.2 8	grain size increased with temperature
[39]	4,2 Wcm^{-2}, sequential	575^0C 5 to 30 min	19 7	3. 60	26.1	0.2 0	Dense surface was observed
[7]	4,2 Wcm^{-2}, sequential	570^0C 20min	21 5	13 .8	25.5	0.7 6	Crakes and pores decrease with preheating duration
[6]	Empirical co-sputtering	520^0C, 560^0C 1 hr	24 3	26 .2	47.9	3.0 5	Large gain size and compact

The second study optimized the sulphurization duration, where the previous study was the optimization of the sulphurization temperature[28]. This study was varied the duration from 5 min to 30 min by taking sulphurization temperature at 575 ^{0}C. The optimized duration 20 min was getting the efficiency of 0.2 % and FF, Voc, Jsc of 0.26, 197 mV, 3.60 mA/cm^2, respectively. The third study investigated a two-step sulphurization method for the sulphurization pre heating time[7]. Hence, this study was followed the two step sequential sulphurization step for the deposition of sample. Firstly, the sample during the time 5 min to 30 min preheated at 250 ^{0}C in (S_2+N_2) atmosphere after that annealed them for 20 min as well as temperature raised up to 570 ^{0}C.

The CTS fabrication film was showed excellent optical properties and good morphology for preheating 15 min duration. Finally, from these three studies, they achieved efficiency 0.76% and FF, Voc and J_{sc} of 0.26, 215 mV, 13.8 mA/cm^2 respectively for the CTS solar cell.

Moreover, another study CuS and SnS target was selected as a precursor using co-sputtering by chierchila et al. [6]. They sulphurized for the deposition at 520 ^{0}C, and 560 ^{0}C during 1 hr in the (S2+N2) atmosphere showed the monochromatic structure and two Ramon shift at 290 cm-1 and 352 cm-1 respectively. Hence, the sample was exhibited large grain size with batter morphology beyond the micrometer range where the ratio Cu/Sn of 1.84 at the salphurized temperature at 520 ^{0}C. The fabricated CTS thin-film solar cell device achieved an efficiency as good as 3.05%, which is the batter value for non –doped, non –alloyed CTS solar cells by a sputtering deposition method.

3) *Pulse lased Deposition (PLD)*

The deposition of CTS thin-film solar cell using PLD technique was used the first time [47]. This study tried to explore the influence of substrate temperature on the deposition rate of CTS and optical properties as well as the electrical properties.

Similarly, Vanalakar et al. was also fabricated CTS thin film using the same PLD technique. This study mixing with SnS_2 and Cu_2S powder by 1/1 molar ratio that was used for the deposition source as well as for the CTS synthesized. The annealing temperatures were at 200 ^{0}C, 300 ^{0}C, and 400 ^{0}C for 1 hr using for the deposition precursor film. The average grain size films were varied from 80 nm to 400 nm, and the annealing temperature was variated 200 ^{0}C to 400 ^{0}C for the CTS polycrystalline cubic phase. The fabricated device was getting higher efficiency of 0.82% at the annealing temperature of 400 0C, with a bandgap of 1.01 eV [14].

B. Non – vacuum deposition technique

The various issues have been suffering in the non-vacuum deposition, which is the barrier to getting a higher efficiency solar cell. Hence, the vacuum methods are costly than the non-vacuum method synthesis processes, which is commercially important.

1) Ball Milling

Ball milling is one of the most commonly used methods for mechanical alloying deposition. It is a simple and economical physical technique as the deposit is carried out in a non-vacuum environment.

Chen et al. (2012) fabricated CTS nanoparticles in a lower milling time of 1 hr where they increased the milling rotation speed up to 800 rpm. The as-deposited samples were annealed in the different temperature range from 350 ^{0}C to 500 ^{0}C. However, the samples annealed at 400 ^{0}C exhibited the highest efficiency of 1.10 %. This team also worked on the modification of p-n junction interface. This term also worked on the improvement of p-n junction of the p-n junction interface. Using In_2S_3 as the n-type buffer layer, the efficiency was further increased up to 1.92%. To obtain batter carrier collection, the p-n junction should be intimate,

smooth, and uniform to ensure the free flow of electrons and holes[17].

High-pressure sintering is employed to enhance the crystallity and achieve a desirable compact microstructure. The application of pressure during the annealing step (5- 50 pa) compresses the grains leading to their merging with other grain, resulting in compact and void-free microstructure [33, 37]. Nomura et al. (2014) synthesized CTS thin films by ball milling followed by post-annealing treatments with high-pressure sintering at 6 MPa followed by subsequent sulfurization. The Cu/Sn ratio 1.9 and post-annealing treatment at 600 0c showed 1.3% efficiency[48]. Neves et al. (2016) succeeded in improving the morphology by using spark plasma sintering (SPS). The sintering was done at 600 0C for 5 min at 50 Mpa, which ensured pure CTS formation. The morphology was found as compact, uniformed, and highly crystalline, which is favourable for solar cell application [49].

2) Solid-State Reaction

In the solid-state reaction method, the predecessors are mixed and reduce the particle size by ball milling to develop an extreme surface area to accelerate the reaction rate. Actually, it is the long-established procedure of fabrication to getting the desire compound. This reaction is a temperature-dependent reaction. To complete this reaction temperature range is 500-1200°C, and it takes two to fifteen days(2- 15days) to complete. The maximum number of researchers have not chosen this method to fabricate thin-film because of the difficulty of controlling the particle size and its surface morphology. The maximum number of reports concerned about the deposition method deals with the thin-film solar cell's structural and electrical properties like CTS. Atomic distribution is their primary focus for CTS compound [45, 48, 50]. The report of Chen et al. (1998) has been described as the process of distribution of Sn and Cu atoms in the tetragonal phase. The report indicates why CTS behaves as a semiconductor, and it has a small number of S-S bonds. Also, Onodo et al. (2000) report shows the distribution of atom in CTS monoclinic compound and also found that it's structure is similar to CuGeSz. Nomura et al. (2013) reduce the bandgap of CTS thin-film 0.8eV to 0.6eV by Se doping. So it clearly indicates that bandgap of CTS can be reduced by doping[48]. Tiwari et al. (2014) used a solid action-reaction method to determine various sulphur effects on CTS solar cell. Among all of the materials only thiourea was capable to produce CTS compound. Thiourea can be attributed future synthesis of CTS [45].

3) Electrodeposition

The sulphurization of the electron deposition process was described for the fabrication of CTS thin-film solar cell by Berg et al.(2012). The CTS monoclinic phase was found from the EDX and XRD investigation, as well as the direct bandgap, was found as 0.93 eV in the bought EQE and PL method. The CTS's final device was getting the value of Voc of 104 mV, Jsc of 17.0 mA/cm^2 and FF of 30.4%, and the efficiency of 0.54%. Therefore, the shunt resistance was measured as 23 Ωcm^2, and the gain EQE was less than 60%. The lower open-circuit voltage was recognized to the lower shunt resistance of the CTS thin film that was the result of the low efficiency [16].

The electrodeposition method was used for CTS monochromatic phase fabrication as well as used Raman analysis by a similar group [16]. The sample preparation was used for necessary electrodepositing metals and sulphurized them at 550 ^{0}C for 2 hr in 500 mbar gas pressure inside a tube furnace.

The highest efficiency of CTS solar cell was achieved in the electrodeposition method by Kokie at al.,(2012). This study analyzed the effect of deposition ratio Cu/Sn on the film properties and varied deposition time to obtain the different ratio of Cu/Sn and the photovoltaic device performance. Therefore, the CTS device was fabricated structure SLG/Mo/CdS/ZnO:Al/Al and the getting efficiency was 2.84% at the ratio Cu/Sn <=2 highest efficiency regarding this electrodeposition method[15].

4) Chemical Bath Deposition

The first CTS thin film was fabricated using the chemical bath deposition technique by Nair et al. (CBD). The sequentially deposited of the CuS and SnS layer using CBD and followed by the annealing in the nitrogen environment for the fabrication of CTS thin film. The CuS layer converted into Cu8S5 at the annealing temperature of 300-340 ^{0}C, which was reacted with the SnS at the 400 ^{0}C. The estimated direct optical band gap was approximately 1eV, whereas, in the dark condition, the electrical conductivity was measured as 1 Ω^{-1}cm^{-1}.

The chemical Bath Deposition processes were studied for the CTS thin film fabrication by the Avellaneda et al. (2010). Hence, the sequential deposition of a 200 nm thick layer of CuS and a 180 nm thick layer of SnS have used CBD method. They were annealed at the 350 ^{0}C and 400 ^{0}C in a nitrogen environment for the film deposition procedure. The fabrication of CTS as Cu2SnS3 and Cu4SnS4 was confirmed using the analysis of grazing X-ray diffraction analysis. The optical band gap was measured by transmittance for Cu_4SnS_4 and Cu_2SnS_3 as 1.2 e V and 0.95 eV, respectively. The CTS thin film was shown as a p-type were as the carrier concentration of 10^{17}-10^{18} cm-3 and the electrical conductivities of 0.5-10 Ω^{-1} cm^{-1}. The generated light's current density was calculated 34 mA/cm^2 and 27 mA/cm^2 for the Cu_2SnS_3 and Cu_4SnS_4, respectively, in the film's 500 nm thickness. The electron-hole pair was 32% and 24% for the Cu_2SnS_3 and Cu_4SnS_4, converting from the optical conversion of solar energy. The buffer layer was used as CdS and CdS/Cu_2SnS_3 and CdS/Cu_4SnS_4 interface were measured as 0.9 eV and 1.1 eV, respectively [24].

IV. CONCLUSION

In conclusion, the CTS solar cell history was reviewed and discussed as the first successful CTS device to present updated research work regarding the field. Therefore, to understand the properties of the material were discussed the characterization of CTS thin film device. To increase the PCE, different Vacuum deposition techniques and Non – vacuum deposition technique are analyzed. The efficiency, FF, short circuit current, and open-circuit voltage were considered for this study. The details were discussed here like compositional, crystal structural, optical, morphological, and electrical properties. The

fundamental properties structure of CTS thin film solar cell was described. The different methodology is also described briefly here for the fabrication of CTS thin-film solar cells. The highest efficiency of the CTS doping with Ge was getting 6.7%[18]. But theoretically, it will forecast 30%. So, the further enhance the CTS performance needs more investigation in the CTS absorber layer to fulfil the future energy demand.

REFERENCES

[1] Tabrizi, A.A. and A. Pahlavan, Efficiency improvement of a silicon-based thin-film solar cell using plasmonic silver nanoparticles and an antireflective layer. Optics Communications, 2020. **454**: p. 124437.

[2] Lokhande, A., et al., *Chemical synthesis of Cu2SnS3 (CTS) nanoparticles: A status review.* Journal of Alloys and Compounds, 2016. **656**: p. 295-310.

[3] Hossain, E.S., et al., Performance assessment of Cu2SnS3 (CTS) based thin film solar cells by AMPS-1D. Current Applied Physics, 2018. **18**(1): p. 79-89.

[4] Lee, T.D. and A.U. Ebong, *A review of thin film solar cell technologies and challenges.* Renewable and Sustainable Energy Reviews, 2017. **70**: p. 1286-1297.

[5] Araki, H., et al., Fabrication of Cu2GeS3-based thin film solar cells by sulfurization of Cu/Ge stacked precursors. Japanese Journal of Applied Physics, 2014. **53**(5S1): p. 05FW10.

[6] Chierchia, R., et al., *Cu2SnS3 based solar cell with 3% efficiency.* physica status solidi (c), 2016. **13**(1): p. 35-39.

[7] Dong, Y., et al., Study on the preheating duration of Cu2SnS3 thin films using RF magnetron sputtering technique for photovoltaics. Journal of Alloys and Compounds, 2016. **665**: p. 69-75.

[8] Tang, Z., et al., Investigation on evaporation and suppression of SnS during fabrication of Cu2SnS3 thin films. physica status solidi (a), 2015. **212**(10): p. 2289-2296.

[9] Aihara, N., et al., Fabrication of Cu2SnS3 thin films by sulfurization of evaporated Cu‐Sn precursors for solar cells. physica status solidi c, 2013. **10**(7‐8): p. 1086-1092.

[10] Chino, K., et al., *Preparation of Cu2SnS3 thin films by sulfurization of Cu/Sn stacked precursors.* Japanese Journal of Applied Physics, 2012. **51**(10S): p. 10NC35.

[11] Kanai, A., et al., Annealing temperature dependence of photovoltaic properties of solar cells containing Cu2SnS3 thin films produced by co‐evaporation. physica status solidi (b), 2015. **252**(6): p. 1239-1243.

[12] Kanai, A., et al., Fabrication of Cu2SnS3 thin-film solar cells with power conversion efficiency of over 4%. Japanese Journal of Applied Physics, 2015. **54**(8S1): p. 08KC06.

[13] Nakashima, M., et al., Cu2SnS3 thin-film solar cells fabricated by sulfurization from NaF/Cu/Sn stacked precursor. Applied Physics Express, 2015. **8**(4): p. 042303.

[14] Vanalakar, S., et al., *Fabrication of Cu2SnS3 thin film solar cells using pulsed laser deposition technique.* Solar Energy Materials and Solar Cells, 2015. **138**: p. 1-8.

[15] Koike, J., et al., *Cu2SnS3 thin-film solar cells from electroplated precursors.* Japanese Journal of Applied Physics, 2012. **51**(10S): p. 10NC34.

[16] Berg, D.M., et al., *Thin film solar cells based on the ternary compound Cu2SnS3.* Thin Solid Films, 2012. **520**(19): p. 6291-6294.

[17] Chen, Q., et al., Study and enhance the photovoltaic properties of narrow-bandgap Cu2SnS3 solar cell by p–n junction interface modification. Journal of colloid and interface science, 2012. **376**(1): p. 327-330.

[18] Umehara, M., et al., *Cu2Sn1− x Ge x S3 solar cells fabricated with a graded bandgap structure.* Applied Physics Express, 2016. **9**(7): p. 072301.

[19] Reddy, T.S., R. Amiruddin, and M.S. Kumar, *Deposition and characterization of Cu2SnS3 thin films by co-evaporation for photovoltaic application.* Solar Energy Materials and Solar Cells, 2015. **143**: p. 128-134.

[20] Su, Z., et al., Fabrication of ternary Cu–Sn–S sulfides by a modified successive ionic layer adsorption and reaction (SILAR) method. Journal of Materials Chemistry, 2012. **22**(32): p. 16346-16352.

[21] Ilari, G.M., et al., *Cu2ZnSnSe4 solar cell absorbers spin-coated from amine-containing ether solutions.* Solar energy materials and solar cells, 2012. **104**: p. 125-130.

[22] Chaudhari, J. and U. Joshi, Fabrication of high quality Cu2SnS3 thin film solar cell with 1.12% power conversion efficiency obtain by low cost environment friendly sol-gel technique. Materials Research Express, 2018. **5**(3): p. 036203.

[23] Fernandes, P., P. Salomé, and A. Da Cunha, *A study of ternary Cu2SnS3 and Cu3SnS4 thin films prepared by sulfurizing stacked metal precursors.* Journal of Physics D: Applied Physics, 2010. **43**(21): p. 215403.

[24] Avellaneda, D., M. Nair, and P. Nair, *Cu2SnS3 and Cu4SnS4 thin films via chemical deposition for photovoltaic application.* Journal of the Electrochemical Society, 2010. **157**(6): p. D346-D352.

[25] Wu, C., et al., Hexagonal Cu 2 Sn S 3 with metallic character: Another category of conducting sulfides. Applied physics letters, 2007. **91**(14): p. 143104.

[26] Zhai, Y.-T., et al., Structural diversity and electronic properties of Cu 2 Sn X 3 (X= S, Se): A first-principles investigation. Physical Review B, 2011. **84**(7): p. 075213.

[27] Shigemi, A., T. Maeda, and T. Wada, *First‐principles calculation of Cu2SnS3 and related compounds.* physica status solidi (b), 2015. **252**(6): p. 1230-1234.

[28] Dong, Y., et al., Effect of sulfurization temperature on properties of Cu2SnS3 thin films and solar cells prepared by sulfurization of stacked metallic precursors. Materials Science in Semiconductor Processing, 2015. **38**: p. 171-176.

[29] Robles, V., et al., Copper tin sulfide (CTS) absorber thin films obtained by co-evaporation: Influence of the ratio Cu/Sn. Journal of Alloys and Compounds, 2015. **642**: p. 40-44.

[30] Fontané, X., et al., In-depth resolved Raman scattering analysis for the identification of secondary phases: Characterization of Cu 2 ZnSnS 4 layers for solar cell applications. Applied Physics Letters, 2011. **98**(18): p. 181905.

[31] Khare, A., et al., First principles calculation of the electronic properties and lattice dynamics of Cu2ZnSn (S1− xSex) 4. Journal of Applied Physics, 2012. **111**(12): p. 123704.

[32] Okano, S., S. Takeshita, and T. Isobe, Formation of Cu2SnS3 nanoparticles by sequential injection of tin and sulfur oleylamine solutions into Cu1. 8S nanoparticle dispersion. Materials Letters, 2015. **145**: p. 79-82.

[33] Bodeux, R., J. Leguay, and S. Delbos, Influence of composition and annealing on the characteristics of Cu2SnS3 thin films grown by cosputtering at room temperature. Thin Solid Films, 2015. **582**: p. 229-232.

[34] Chalapathi, U., et al., Effect of annealing on the structural, microstructural and optical properties of co-evaporated Cu2SnS3 thin films. Vacuum, 2015. **117**: p. 121-126.

[35] Matsumoto, Y., et al., Preparation of monoclinic Cu2SnS3 single crystal by chemical vapor transport with iodine. Materials Letters, 2016. **170**: p. 213-216.

[36] Nakashima, M., et al., Cu2SnS3 thin film solar cells prepared by thermal crystallization of evaporated Cu/Sn precursors in sulfur and tin atmosphere. physica status solidi (c), 2015. **12**(6): p. 761-764.

[37] Zhang, H., et al., Fabrication of highly crystallized Cu2SnS3 thin films through sulfurization of Sn-rich metallic precursors. Journal of Alloys and compounds, 2014. **602**: p. 199-203.

[38] Kuku, T.A. and O.A. Fakolujo, Photovoltaic characteristics of thin films of Cu2SnS3. 1987.

[39] Dong, Y., et al., Synthesis and optimized sulfurization time of Cu2SnS3 thin films obtained from stacked metallic precursors for solar cell application. Materials Letters, 2015. **160**: p. 468-471.

[40] Aihara, N., et al., Sulfurization temperature dependences of photovoltaic properties in Cu2SnS3-based thin-film solar cells. Japanese Journal of Applied Physics, 2014. **53**(5S1): p. 05FW13.

[41] Baranowski, L.L., et al., *Control of doping in Cu2SnS3 through defects and alloying.* Chemistry of Materials, 2014. **26**(17): p. 4951-4959.

[42] Bouaziz, M., M. Amlouk, and S. Belgacem, *Structural and optical properties of Cu2SnS3 sprayed thin films.* Thin Solid Films, 2009. **517**(7): p. 2527-2530.

[43] Bouaziz, M., et al., Growth of Cu2SnS3 thin films by solid reaction under sulphur atmosphere. Vacuum, 2011. **85**(8): p. 783-786.

[44] Tiwari, D., et al., Non-toxic, earth-abundant 2% efficient Cu2SnS3 solar cell based on tetragonal films direct-coated from single metal-organic precursor solution. Solar Energy Materials and Solar Cells, 2013. **113**: p. 165-170.
[45] Tiwari, D., T.K. Chaudhuri, and T. Shripathi, Electrical transport in layer-by-layer solution deposited Cu2SnS3 films: Effect of thickness and annealing temperature. Applied Surface Science, 2014. **297**: p. 158-166.
[46] Umehara, M., et al., Cu2Sn1-xGexS3 (x= 0.17) thin-film solar cells with high conversion efficiency of 6.0%. Applied Physics Express, 2013. **6**(4): p. 045501.
[47] Ettlinger, R.B., et al., *Pulsed laser deposition from ZnS and Cu2SnS3 multicomponent targets.* Applied Surface Science, 2015. **336**: p. 385-390.
[48] Nomura, T., T. Maeda, and T. Wada, *Preparation of narrow band-gap Cu2Sn (S, Se) 3 and fabrication of film by non-vacuum process.* Japanese Journal of Applied Physics, 2013. **52**(4S): p. 04CR08.
[49] Neves, F., J. Correia, and K. Hanada, *Spark plasma sintering of Cu2SnS3 powders synthesized by mechanical alloying.* Materials Letters, 2016. **164**: p. 165-168.
[50] Di Benedetto, F., et al., *Preliminary XAS investigations on some phases of the Cu‐Sn‐S system.* physica status solidi c, 2013. **10**(7‐8): p. 1055-1057.